UDK 544.537:57.012.3:539.536
Original scientific article/Izvirni znanstveni članek

ISSN 1580-2949
Mater. Tehnol.

EFFECTS OF LASER POWER, SCAN SPEED AND HEAT TREATMENT ON MICROSTRUCTURE AND HARDNESS OF PBF-LB INCONEL 718

VPLIV MOČI LASERJA, HITROSTI SKENIRANJA IN TOPLOTNE OBDELAVE NA MIKROSTRUKTURO IN TRDOTO IZDELKOV IZ SUPERZLITINE INCONEL 718 IZDELANE Z LASERSKIM NATALJEVANJEM

Ahmed W. Abdelghany[1,2*], Matias Jaskari[1], Sami Westman[3], Ilkka Poutiainen[3], Antti Järvenpää[1,3]

[1]Future Manufacturing Technologies (FMT), Kerttu Saalasti Institute, University of Oulu, Nivala 85500, Finland
[2]Design and Production Engineering Dept., Faculty of Engineering, Ain Shams University, Cairo 11535, Egypt
[3]Laser Processing and Additive Manufacturing, Mechanical Engineering Department, School of Energy Systems, Lappeenranta-Lahti University of Technology, LUT, P.O. Box 20, FI-53851, Lappeenranta, Finland

Prejem rokopisa – received: 2025-10-03; sprejem za objavo – accepted for publication: 2026-01-26

doi:10.17222/mit.2025.1581

This study quantifies the effects of laser power and scan speed on the aged microstructure and hardness of PBF-LB Inconel 718 processed under the EOS-standard heat-treatment schedule. Cylindrical specimens were fabricated on an EOS M290 using six power–speed combinations spanning a line energy ($E_{line} = P/v$) range of 0.167–0.583 J·mm^{-1}, followed by solution annealing and double ageing according to the EOS recommendation. Microstructure was assessed by EBSD, and hardness was measured in both the as-built and aged conditions. EBSD revealed build-direction-aligned columnar γ grains under all conditions, while increasing line energy was associated with a progressively coarser boundary/subgrain network. The lowest line-energy (highest scan-speed) condition (200 W/1200 mm·s^{-1}; 0.167 J·mm^{-1}) achieved the highest post-age hardness (≈459 HV5), whereas the highest line-energy condition (350 W/600 mm·s^{-1}; 0.583 J·mm^{-1}) exhibited the lowest hardness (≈438 HV5) together with void-like, non-indexed features consistent with porosity. Overall, the results provide a compact process–structure–property map and energy-aware guidance for selecting PBF-LB Inconel 718 parameter windows, highlighting that while lower line-energy conditions maximise performance, higher-speed regimes may still deliver sufficient quality for short-life or productivity-driven components.

Keywords: additive manufacturing, PBF-LB, Inconel 718, laser power, scan speed, line energy, heat treatment

Avtorji v članku opisujejo študijo vpliva moči laserja in hitrosti skeniranja na mikrostrukturo in trdoto izdelkov iz starane superzlitine Inconel 718, izdelanih s postopkom laserskega nataljevanja »posteljice« iz kovinskega prahu (PBF-LB; angl.: Laser powder bed fusion). To je tako imenovano 3D tiskanje s postopkom direktnega nataljevanja/sintranja kovine z laserjem plast za plastjo (DMLS, angl.: Direct Metal Laser Melting/Sintering). Izdelane preizkušance so naknadno toplotno obdelali s standardnim postopkom podjetja EOS GmbH. Valjaste vzorce so izdelali na stroju EOS M290 z uporabo šestih kombinacij moči in hitrosti v območju energije črt ($E_{line} = P/v$) od 0,167 do 0,583 J·mm^{-1}, nato pa so izdelane vzorce raztopno žarili in dvakrat starali v skladu s priporočilom podjetja EOS. Mikrostrukturo vzorcev so avtorji ocenili s pomočjo metode povratno sipanih elektronov (EBSD; angl.: Electron backscatter diffraction). Njihovo trdoto pa so izmerili tako v izdelanem (3 D printanem) kot tudi staranem stanju. Z EBSD tehniko so avtorji odkrili mikrostrukturo s stebrastimi $\bar{\alpha}$ zrni, poravnanimi s smerjo izdelave, pri vseh pogojih, medtem ko je bila naraščajoča energija črt povezana z napredujočo bolj grobo mrežo mej in podzrn. Uporaba najnižje linijske energije oziroma najvišje hitrosti skeniranja (200 W/1200 mm·s^{-1}; 0,167 J·mm^{-1}) je dala najvišjo trdoto vzorcev po staranju (≈459 HV5), medtem ko se je uporaba najvišje linijske energije (350 W/600 mm·s^{-1}; 0,583 J·mm^{-1}) odražala v najnižji trdoti vzorcev (≈438 HV5) skupaj s prazninam podobnimi in neindeksiranimi artefakti, kar je skladno z izmerjeno poroznostjo. Na splošno rezultati uporabljenega načina izdelave vzorcev zagotavljajo kompakten zemljevid (angl.: map) *proces-struktura-lastnosti* in energijsko optimizirana navodila za izbiro parametrskih oken za PBF-LB izdelavo izdelkov iz superzlitine Inconel 718. Avtorji v zaključkih povdarjajo, da uporaba pogojev z nižjo linijsko energijo omogoča maksimalno zmogljivost. Režimi z višjo hitrostjo pa še vedno lahko zagotavljajo zadostno kakovost komponent (izdelkov) s kratko življenjsko dobo ali tistih, ki so namenjen za veliko serijsko proizvodnjo.

Ključne besede: proizvodnja z dodajalno tehnologijo, Inconel 718, laserska moč, hitrost skeniranja, linijska energija, toplotna obdelava

1 INTRODUCTION

Laser powder bed fusion (PBF-LB) builds metallic parts by spreading and selectively melting thin powder layers with a scanning laser, enabling complex shapes with minimal downstream machining, an advantage for difficult-to-machine alloys such as Inconel 718 (IN718). However, the local thermal gradients inherent to PBF-LB produce residual stress and a nonequilibrium solidification structure. In IN718, the as-built state typically shows columnar γ grains aligned with the build direction (BD), cellular substructure, and a weak-to-moderate texture aligned with the build directions.[1]

*Corresponding author's e-mail:
ahmed.abdelghany@oulu.fi (Ahmed W. Abdelghany)

Defect formation further complicates property control. Pores arise from several factors; for instance, a lack of fusion when remelting is insufficient, and keyhole/overheating when the heat input is excessive, each with distinct morphologies and process conditions. Consequently, energy-density descriptors can produce different melt-pool behaviours, and therefore cannot, by themselves, ensure a defect-free build.[2] Post-build heat treatment is therefore essential. Industrial practice (e.g., the EOS schedule) applies solution annealing at 954 °C for 1 h (air/argon cool), followed by double ageing at 718 °C for 8 h, furnace-cooling to 621 °C, and holding for a total of 18 h before air cooling. The intent is to precipitate the primary γ" (Ni_3Nb) and secondary γ' (Ni_3 (Al, Ti)) phases and to relieve stresses.[3,4] This ageing route reliably produces a precipitation-strengthened state with hardness in the high-400 HV range, as reported in validated data sheets. The precipitation of coherent γ" dominates the age-hardening response of AM-IN718.

Kinetics studies quantify accelerated hardening from the as-built state and activation energies consistent with Nb diffusion, explaining rapid hardness rise during 700–800 °C ageing.[4] At the same time, process parameters (laser power and scan speed) independently influence melt-pool geometry, texture, and substructure, and hence the subsequent precipitation response, even when nominal energy input is similar.[5,6] Rapid solidification in PBF-LB can introduce microstructural heterogeneities (e.g., Laves-phase segregation) and defects (e.g., porosity) that reduce the as-built mechanical performance.[7,8] As identical volumetric energy density values can yield varying porosity and microstructures under different laser parameter combinations, the relationships between LPBF processing conditions, microstructure evolution, and the mechanical performance of IN718 remain insufficiently understood and require further investigation.[8,9]

The present study constructs a compact process–structure–property map for PBF-LB IN718 built on an EOS M290, using six laser power–scan-speed combinations at fixed hatch spacing and layer thickness, all subjected to the EOS-standard ageing schedule. Microstructure (EBSD) and hardness were measured and compared for all conditions in both as-built and heat-treated states. In addition to identifying process windows for optimal structural performance, the results clarify the trade-off between achieving defect-free, high-reliability components and enabling faster build rates for short-life or non-critical parts, where moderate microstructural degradation may be acceptable.

2 EXPERIMENTAL PART

2.1 Materials, build design, and heat treatment

PBF-LB fabricated cylindrical specimens of IN718 (EOS NickelAlloy IN718 powder) on an EOS M290, and the geometry is shown in **Figure 1a**. The feedstock was a pre-alloyed, gas-atomised Inconel 718 powder supplied by EOS (EOS NickelAlloy IN718). According to the supplier's specification/certificate, the powder particle-size distribution ranged from ≈20 to ≈63 μm, and the particles exhibited a predominantly spherical morphology typical of gas-atomised powders. The nominal chemical composition of the EOS IN718 powder (*w*/%) was Ni 50–55, Cr 17–21, Nb 4.75–5.50, Mo 2.80–3.30, Ti 0.65–1.15, Al 0.20–0.80, Fe balance, with minor elements within the supplier limits.[3] Cylindrical specimens were printed using a bi-zone build design (**Figure 1b**): the lower 5 mm section was fabricated using the EOS reference parameter set, while the upper 5 mm section was fabricated using one of the investigated power–speed parameter sets (**Table 1**). This design enables within-specimen comparison under identical build orientation and subsequent heat-treatment history. Hatch spacing (h) and layer thickness (t) were held constant (following EOS recommended values). With h and t fixed, the volumetric energy density $VED = P/(v{\cdot}h{\cdot}t)$ is proportional to the line energy ($E_{line} = P/v$), where P is the laser power, and v is the laser speed.[9] As a rational index of relative heat input per scan length, E_{line} was used to order the conditions for comparison and discussion. Five custom P–v conditions and one EOS reference were investigated and summarised in **Table 1**. For comparability, we report line energy = P/v (J·mm^{-1}) as an ordering index of heat input per unit scan length. The power and scan-speed conditions were designed to span the practical heat-input window on the EOS M290, covering both low and high line-energy extremes, while including the EOS default condition as a mid-range benchmark. Two additional intermediate conditions were included to capture a monotonic trend with line energy under fixed hatch spacing and layer thickness.

Table 1: PBF-LB various process parameters used for printing the test specimens

	Laser power (W)	Laser speed (mm·s^{-1})	E_{line} (J·mm^{-1})
E1	200	1200	0.167
E2	200	1100	0.182
E3*	285	960	0.297
E4	350	700	0.500
E5	350	600	0.583
E_{ref}	EOS standard		

*Default known parameters for EOS PBF-LB

All specimens underwent the EOS-standard heat treatment schedule for IN718 (**Figure 1b**). The heat treatment comprised solution annealing at ≈954 °C for 1 h followed by air cooling, then a double-ageing cycle, 718 °C for 8 h, furnace-cooling to 621 °C, holding at 621 °C until a total ageing time of 18 h, and air (or argon) cooling. Heat treatments were performed in a Nabertherm LH 120/12 laboratory chamber furnace. The solution treatment partially relieves stress in the PBF-LB-built material and reduces segregation-related heterogeneity.[10] On the other hand, the double ageing

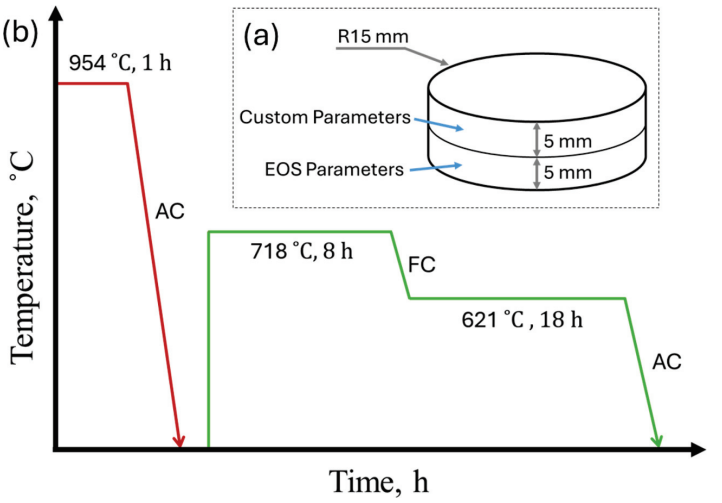

Figure 1: a) Geometry of the PBF-LB fabricated sample prior to heat treatment, b) schematic of the EOS-standard ageing heat treatment schedule applied to all specimens

treatment drives precipitation of the principal strengthening phases, γ" and γ', which leads to a marked increase in hardness and associated mechanical performance.[11]

2.2 Microstructure characterisation and hardness measurements

Longitudinal cross-sections containing the build direction (BD) were prepared for EBSD by metallographic grinding and polishing to obtain a deformation-minimised surface suitable for Kikuchi-pattern acquisition. Specimens were ground sequentially using SiC papers up to fine grits, followed by a final oxide polish (colloidal silica). EBSD was performed on a field-emission SEM (JEOL JSM-7900F) equipped with an Oxford Instruments EBSD detector and AZtec-Crystal software, with maps acquired at 15 kV and a step size of 1 µm.

Vickers hardness was measured in the as-built and aged states on a Struers DuraScan 70 at HV5, with ≥5 indents per half (custom-parameter half and EOS-parameter half) per specimen.

3 RESULTS AND DISCUSSION

Across the six power–speed conditions, the EOS-standard ageing (954 °C/1 h + double aging) raised hardness from ≈295–315 HV (as-built) to ≈438–459 HV (aged). The hardness measurement results for all conditions are shown in **Figure 2**. The results showed that the lowest line-energy condition, E1 (200 W/1200 mm·s^{-1}), achieved the highest hardness (≈459 HV). In contrast, the highest line-energy condition, E5 (350 W/600 mm·s^{-1}), exhibited the lowest hardness (≈438 HV), and the EOS reference condition lay in between (≈447 HV). This level and spread are consistent with the EOS datasheet values for heat-treated IN718 under the same schedule and they indicate that γ"/γ' precipitation dominates the absolute hardness after ageing, while build-condition effects shift it within a relatively narrow band. The EOS documentation explicitly describes this schedule and its intent (γ" as the primary strengthening phase), which aligns with our observation that post-age hardness across all conditions falls within a tight window.[12] Quantitatively, precipitation strengthening has been shown to be the largest single contributor to strength in PBF-LB IN718 subjected to direct ageing or to homogenization followed by ageing; dislocation, grain-boundary, and solution strengthening contribute less to the total increment. Thus, modest hardness differences among identically aged builds plausibly arise from the as-built substructure's mediation of γ"/γ' precipitation

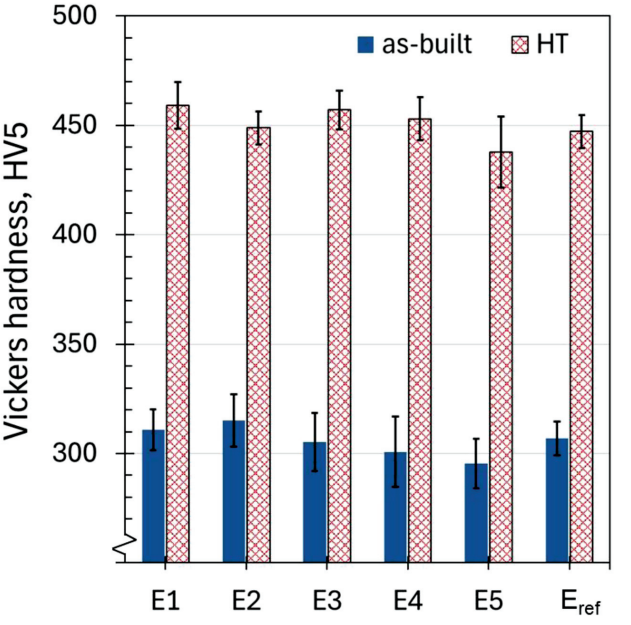

Figure 2: Comparison of Vickers hardness (HV5) between the as-built and heat-treated (HT) conditions for all evaluated process parameters (E1 to E5 and reference sample E_{ref})

during ageing.[12] Laser power and scan speed have independent effects on precipitation and final properties even at similar energy densities.[7] Even under identical standard heat treatment, final properties of LPBF IN718 can differ because the laser power–scan speed history influences precipitation behaviour through its effect on the thermal history, grain structure, and solute distribution.[7] Studies have shown that signatures of the original LPBF process, such as texture and segregation patterns, can persist after heat treatment and continue to affect mechanical properties.[13]

The microstructure investigation via EBSD for all the heat-treated conditions (**Figure 3**) shows the expected elongated, build-direction (BD)-aligned grains from directional solidification. The columnar grains with a cellular substructure and likely high dislocation density are characteristic of as-built IN718 and persist after ageing.[12] Within this study, E1 (200 W/1200 mm·s^{-1}) exhibits the finest grain/subgrain among the tested conditions, while E5 (350 W/600 mm·s^{-1}) appears coarser along BD. Moreover, E3 (285 W/960 mm·s^{-1}) exhibits a microstructure closely matching the EOS reference (E_{ref}), consistent with E3 being the default printing condition, and their aged hardness values of 457 HV and 447 HV, respectively. A finer boundary/subgrain network is expected to indirectly assist precipitation hardening (by providing more nucleation sites/shorter diffusion paths), consistent with the higher post-age hardness observed for E1 relative to E5. Previous studies indicate that volumetric or line energy is only a first-order descriptor, where different power–speed pairs at the same nominal energy can fall into distinct porosity regimes.[2] Even when relative density is high, residual pores reduce strength and ductility; thus, the coarser BD-aligned grain structure together with porosity in E5 is consistent with its lower performance.[2,14] The EOS-standard ageing presumably

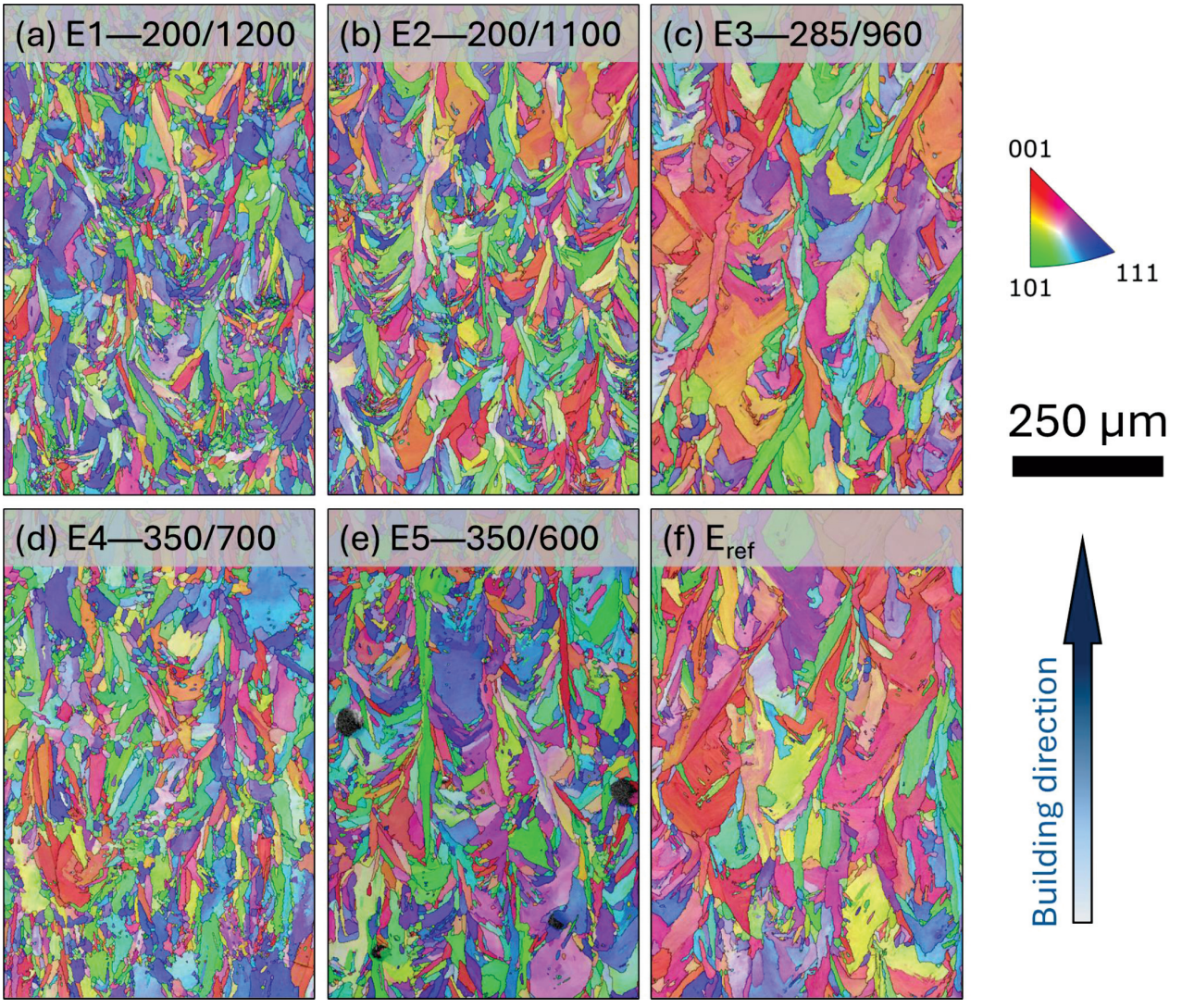

Figure 3: EBSD inverse pole figure orientation maps for the heat-treated PBF-LB Inconel-718, ordered by increasing line energy (E_{line}): a) E1: 200 W/1200 mm·s^{-1}, b) E2: 200 W/1100 mm·s^{-1}, c) E3: 285 W/960 mm·s^{-1}, d) E4: 350 W/700 mm·s^{-1}, e) E5: 350 W/600 mm·s^{-1}, f) EOS reference parameters (E_{ref})

drives all builds into a precipitation-strengthened state in which γ''/γ' dominates the hardness, yielding a narrow range of 438–459 HV. Lower line-energy (higher-speed) settings (e.g., E1) retain a finer-grained network and correspondingly achieve the highest hardness, whereas the highest line-energy case (E5) shows a coarser boundary network together with occasional void-like (non-indexed) features and therefore lies at the lower end of the hardness range, consistent with the literature.[7,9]

4 CONCLUSIONS

The present study examines PBF-LB IN718 built in six power–speed sets under both as-built and heat-treated conditions, focusing on the links between microstructure and hardness. All six PBF-LB IN718 builds showed a significant increase in hardness after EOS-standard solution annealing and double ageing, rising from ≈295–315 HV in the as-built state to ≈438–459 HV in the aged state. The sample processed with the lowest line energy (E1: 200 W at 1200 mm/s, 0.167 J/mm) attained the highest aged hardness (459 HV), whereas the highest line-energy condition (E5: 350 W at 600 mm/s, 0.583 J/mm) yielded the lowest aged hardness (438 HV). EBSD mapping revealed columnar grains aligned with the build direction in all conditions. The subgrain structure depended on the applied line energy: the lowest line-energy build (E1) exhibited finer subgrains, while the highest line-energy build (E5) produced coarser subgrains along with void-like non-indexed regions. Such defects can reduce the ductility and fatigue resistance and should be avoided during parameter selection. These results confirm that the line energy (P/v) is an effective metric for ordering the process parameters (with fixed hatch spacing and layer thickness) and correlating them with the resulting microstructural refinement and hardness after standard post-processing.

Acknowledgment

Support from the Laser Laboratory at the LUT University and the FMT Group, University of Oulu, is gratefully acknowledged for providing research facilities.

5 REFERENCES

[1] G. Kasperovich, J. Gussone, G. Requena, N. Schell, A. Stark, J. Haubrich, Tailoring the strength of Inconel 718: Insights into LPBF parameters and heat-treatment synergy, Mater. Des., 250 (**2025**), 113627, doi:10.1016/j.matdes.2025.113627

[2] C. Smith, G. Hommer, M. Keeler, J. Gockel, K. Findley, C. Brice, A. Clarke, J. Klemm-Toole, Assessing volumetric energy density as a predictor of defects in laser powder bed fusion 316L stainless steel, JOM, 77 (**2025**), 737–748, doi:10.1007/s11837-024-06946-z

[3] EOS NickelAlloy IN718 Material Data Sheet, online: https://www.eos.info/var/assets/05-datasheet-images/Assets_MDS_Metal/EOS_NickelAlloy_IN718/Material_DataSheet_EOS_NickelAlloy_IN718_en.pdf?v=3

[4] S. Ghaemifar, H. Mirzadeh, Precipitation kinetics of gamma double prime phase during direct aging treatment of Inconel 718 superalloy additively manufactured by selective laser melting, J. Mater. Res. Technol., 27 (**2023**), 4248–4255, doi:10.1016/j.jmrt.2023.10.267

[5] N. Ghanadi, K. Son, M. Alvarado, S. Yang, H. M. Kao, C. H. Chang, B. K. Paul, S. Pasebani, Effect of LPBF processing parameters on Inconel 718 lattice structures: Geometrical characteristics, surface morphology, and mechanical properties, Mater. Des., 253 (**2025**), 113864, doi:10.1016/j.matdes.2025.113864

[6] H. Liu, W. Cheng, Y. Sun, R. Ma, Y. Wang, J. Bai, L. Xue, X. Song, C. Tan, Effects of process parameters and heat treatment on microstructure and mechanical characteristics of laser powder bed fusion alloy Inconel 718, Coatings, 13 (**2023**) 189, doi:10.3390/coatings13010189

[7] H. Pan, T. Dahmen, M. Bayat, K. Lin, X. Zhang, Independent effects of laser power and scanning speed on IN718's precipitation and mechanical properties produced by LPBF plus heat treatment, Mater. Sci. Eng. A, 849 (**2022**), 143530, doi:10.1016/j.msea.2022.143530

[8] Y. Guo, S. Wu, X. Yan, W. Jiang, B. Zhu, H. Qiu, Z. Liu, Defects, microstructure and associated mechanical properties of Inconel 718 fabricated by selective electron beam melting, J. Alloys Compd., 1006 (**2024**), 176279, doi:10.1016/j.jallcom.2024.176279

[9] G. V. de Leon Nope, L. I. Perez-Andrade, J. Corona-Castuera, D. G. Espinosa-Arbelaez, J. Muñoz-Saldaña, J. M. Alvarado-Orozco, Study of volumetric energy density limitations on the IN718 microstructure in laser powder bed fusion process, J. Manuf. Process., 64 (**2021**), 1261–1272, doi:10.1016/j.jmapro.2021.02.043

[10] R. Sun, W. Li, Y. Zhang, T. Hu, P. Wang, Effect of solution treatment on high-temperature mechanical properties of IN718 manufactured by selective laser melting, J. Mater. Eng. Perform., 30 (**2021**), 6821–6831, doi:10.1007/s11665-021-06024-4

[11] C. Slama, M. Abdellaoui, Precipitation kinetics of γ' and γ'' particles in Inconel 718 and its influence on mechanical properties, Mater. Today Commun., 38 (**2024**), 108158, doi:10.1016/j.mtcomm.2024.108158

[12] S. Zhang, X. Lin, L. Wang, X. Yu, Y. Hu, H. Yang, L. Lei, W. Huang, Strengthening mechanisms in selective laser-melted Inconel 718 superalloy, Mater. Sci. Eng. A, 812 (**2021**), 141145, doi:10.1016/j.msea.2021.141145

[13] T. D. McLouth, D. B. Witkin, G. E. Bean, S. D. Sitzman, P. M. Adams, J. R. Lohser, Variations in ambient and elevated temperature mechanical behavior of IN718 manufactured by selective laser melting via process parameter control, Mater. Sci. Eng. A, 780 (**2020**), 139184, doi:10.1016/j.msea.2020.139184

[14] M. Khedr, K. Elkhouly, M. Jaskari, M. A. J. Finnilä, A. Järvenpää, A. W. Abdelghany, Role of printing density in internal defect evolution and hydrogen embrittlement of PBF-LB 316L stainless steel fabricated from recycled powder, Mater. Des., 257 (**2025**), 114506, doi:10.1016/j.matdes.2025.114506